Cellular and Molecular Life Sciences (2020) 77:331–350
https://doi.org/10.1007/s00018-019-03184-4

ORIGINAL ARTICLE

Degradome of soluble ADAM10 and ADAM17 metalloproteases

Franka Scharfenberg[1] · Andreas Helbig[2] · Martin Sammel[1] · Julia Benzel[3] · Uwe Schlomann[3] · Florian Peters[1] · Rielana Wichert[1] · Maximilian Bettendorff[1] · Dirk Schmidt-Arras[4] · Stefan Rose-John[4] · Catherine Moali[5] · Stefan F. Lichtenthaler[6,7,8] · Claus U. Pietrzik[9] · Jörg W. Bartsch[3] · Andreas Tholey[2] · Christoph Becker-Pauly[1]

Received: 4 December 2018 / Revised: 10 May 2019 / Accepted: 6 June 2019 / Published online: 17 June 2019

Abstract

Disintegrin and metalloproteinases (ADAMs) 10 and 17 can release the extracellular part of a variety of membrane-bound proteins via ectodomain shedding important for many biological functions. So far, substrate identification focused exclusively on membrane-anchored ADAM10 and ADAM17. However, besides known shedding of ADAM10, we identified ADAM8 as a protease capable of releasing the ADAM17 ectodomain. Therefore, we investigated whether the soluble ectodomains of ADAM10/17 (sADAM10/17) exhibit an altered substrate spectrum compared to their membrane-bound counterparts. A mass spectrometry-based N-terminomics approach identified 134 protein cleavage events in total and 45 common substrates for sADAM10/17 within the secretome of murine cardiomyocytes. Analysis of these cleavage sites confirmed previously identified amino acid preferences. Further in vitro studies verified fibronectin, cystatin C, sN-cadherin, PCPE-1 as well as sAPP as direct substrates of sADAM10 and/or sADAM17. Overall, we present the first degradome study for sADAM10/17, thereby introducing a new mode of proteolytic activity within the protease web.

Keywords TAILS · ADAM8 · ADAM10 · ADAM17 · Ectodomain shedding · Proteolysis

Abbreviations

ACN	Acetonitrile
ADAM	A disintegrin and metalloprotease
APP	Amyloid precursor protein
CTF	C-terminal fragment
DAPT	*N*-[*N*-(3,5-Difluorophenacetyl)-L-alanyl]-*S*-phenylglycine *t*-butyl ester
DCM	Dilated cardiomyopathy
dnp	2,4-Dinitrophenyl
ECM	Extracellular matrix
FCS	Fetal calf serum
HEK	Human embryonic kidney
LC–MS/MS	Liquid chromatography–tandem mass spectrometry
Mca	7-Methyloxycoumarin-4-yl-acetyl
MMP	Matrix metalloproteinase
PCPE-1	Procollagen C-proteinase enhancer-1
PSM	Peptide scoring matches
RFU	Relative fluorescence unit

Electronic supplementary material The online version of this article (https://doi.org/10.1007/s00018-019-03184-4) contains supplementary material, which is available to authorized users.

✉ Franka Scharfenberg
fscharfenberg@biochem.uni-kiel.de

✉ Christoph Becker-Pauly
cbeckerpauly@biochem.uni-kiel.de

1 Unit for Degradomics of the Protease Web, Biochemical Institute, University of Kiel, Kiel, Germany

2 Systematic Proteomics and Bioanalytics, Institute for Experimental Medicine, University of Kiel, Kiel, Germany

3 Department of Neurosurgery, Philipps University Marburg, Marburg, Germany

4 Biochemical Institute, University of Kiel, Kiel, Germany

5 Tissue Biology and Therapeutic Engineering Unit, LBTI, UMR 5305, Univ. Lyon, Université Claude Bernard Lyon 1, CNRS, 69367 Lyon, France

6 Neuroproteomics, School of Medicine, Klinikum rechts der Isar, Institute for Advanced Study, Technical University Munich, Munich, Germany

7 Munich Center for Systems Neurology (SyNergy), Munich, Germany

8 German Center for Neurodegenerative Diseases (DZNE), Munich, Germany

9 Institute for Pathobiochemistry, University Medical Center of the Johannes Gutenberg-University Mainz, Mainz, Germany

SD	Standard deviation
TAILS	Terminal amine isotopic labeling of substrates
TCA	Trichloracetic acid
TFA	Trifluoroacetic acid
TIMP	Tissue inhibitor of metalloproteinases
TMT	Tandem mass tag
TR	Technical replicate

Introduction

The proteolytic release of soluble extracellular mediators is crucial for almost all biological processes, from embryonic development and tissue homeostasis to cell death [1–4]. Dysregulation of ectodomain shedding is associated with several pathologies, demonstrating the importance of such irreversible proteolytic events [1, 5]. Members of a disintegrin and metalloproteinase (ADAM) family are known to mediate ectodomain shedding of a variety of membrane-bound proteins affecting cell adhesion, migration, signaling, and proteolysis [2, 6–9].

The ubiquitously expressed membrane-bound proteases ADAM10 and ADAM17 are the most intensively studied and best characterized members of the ADAM proteinase family. With regard to sequence homology and structure, these two proteases are closely related to each other and set apart from all other ADAMs [6]. A characteristic feature is the unique domain composition within the ADAM family comprising an N-terminal signal peptide followed by a prodomain, a metalloprotease domain, a disintegrin domain, a cysteine-rich domain, a single transmembrane helix, and a cytoplasmic region [10]. Several studies confirmed a number of specific substrates for ADAM10 (e.g., N-cadherin and betacellulin) or ADAM17 (e.g., TNFα, amphiregulin, and HB-EGF), but also unraveled overlapping specificities (e.g., IL-6R, Notch, and APP) [11–13], suggesting compensatory proteolytic activities regulated in a cell type- and tissue-dependent manner. The broad and complex spectrum of shedding substrates has characterized ADAM10 and ADAM17 as important molecular switches of major physiological pathways controlling tissue regeneration, inflammatory immune responses, cancer development, neurodegenerative pathologies, and cardiovascular diseases [12, 14–16].

The analysis of loss-of-function mouse models revealed that ADAM10 and ADAM17 are essential for organ development and that deficiency leads to embryonic lethality [17, 18]. The severe morphological defects affect various tissues including the heart [17–19]. Here, the absence of functional ADAM10 or ADAM17 leads to severely impaired cardiac development [18, 20–22]. Altered expression levels in response to specific heart pathologies such as myocarditis [23], different cardiomyopathies [24], atrial fibrillation [25], or myocardial infarction [26, 27] reflect the impact of ADAM10 and ADAM17 for structural integrity and remodeling of cardiac tissue.

Fig. 1 ADAM8-dependent shedding of ADAM17. **a** Immunoblot of MDA-MB-231 ADAM8 knockout (hA8 ko) and control (ctrl) cell lysates. **b** Relative increased soluble protein levels of MDA-MB-231 ctrl vs hA8 ko clones determined by the soluble receptor array are shown. **c** ELISA OD levels corresponding to the amount of soluble ADAM17 in conditioned cell-culture medium of MDA-MB-231 hA8 ko and ctrl clones. **d** Immunoblot of the Co-IP assay. Cell lysates of MDA-MB-231 hA8 ko clone transfected with a human ADAM8 Flag tag expression construct was loaded on magnetic beads covalently coupled with a Flag tag ab or mouse IgG. Shown is the signal of ADAM8 and ADAM17 (arrows indicate the pro and mature form of ADAM17) in the cell lysates and in the eluted fraction. **e** Shedding of ADAM17 in ADAM10$^{-/-}$; 17$^{-/-}$ HEK293T cells transfected with mADAM17 and/or mADAM8, monitored by immunoblotting. Shedding of mADAM17 was analyzed in ultracentrifuged, TCA precipitated supernatants (*) with an antibody raised against the ectodomain and in the lysate based on the enrichment of CTFs, detected with an ADAM17 C-terminal specific antibody. BB-94, BK-13-61, or GW was added to the medium 24 h before collecting the supernatants. Cells were additionally treated with DAPT to inhibit y-secretase. **f** Co-immunoprecipitation of mADAM8 and mADAM17. ADAM10$^{-/-}$; 17$^{-/-}$ HEK293T cells were transfected with a C-terminal Myc-tagged mADAM8 and/or mADAM17. ADAMs were immunoprecipitated via the Myc-tag and proteins analyzed by immunoblotting

Interestingly, in human dilated cardiomyopathy (DCM), ADAM15 expression was found to be increased [24]. ADAM15 again is a sheddase of ADAM10 [28], which potentially results in elevated levels of soluble shed ADAM10 in the cardiac extracellular matrix (ECM). For ADAM17, no particular sheddase has been described so far. However, cell-culture experiments demonstrated that ADAM17 can undergo shedding [29], which is further supported by several reports on ADAM17 activity in plasma [30, 31].

Based on these observations and our identification of ADAM8 as a sheddase of ADAM17, we hypothesized that the shedding of ADAM10 and ADAM17 is not only a mechanism to downregulate cell-surface activity of these proteases, but instead enables soluble ADAM10 and ADAM17 (sADAM10/17) to get access to a so far not characterized substrate pool of soluble proteins. To address this issue, we employed a mass spectrometry-based proteomics approach [32] to identify substrates for sADAM10 and sADAM17 in the secretome of murine cardiomyocytes and additionally verified shedding activities of the soluble proteases toward known targets of membrane-bound ADAM10 and ADAM17.

Results

ADAM17 is shed by ADAM8

Recently, it was shown that an ADAM8 dependent shedding of the P-selectin ligand PSGL-1 regulates transendothelial

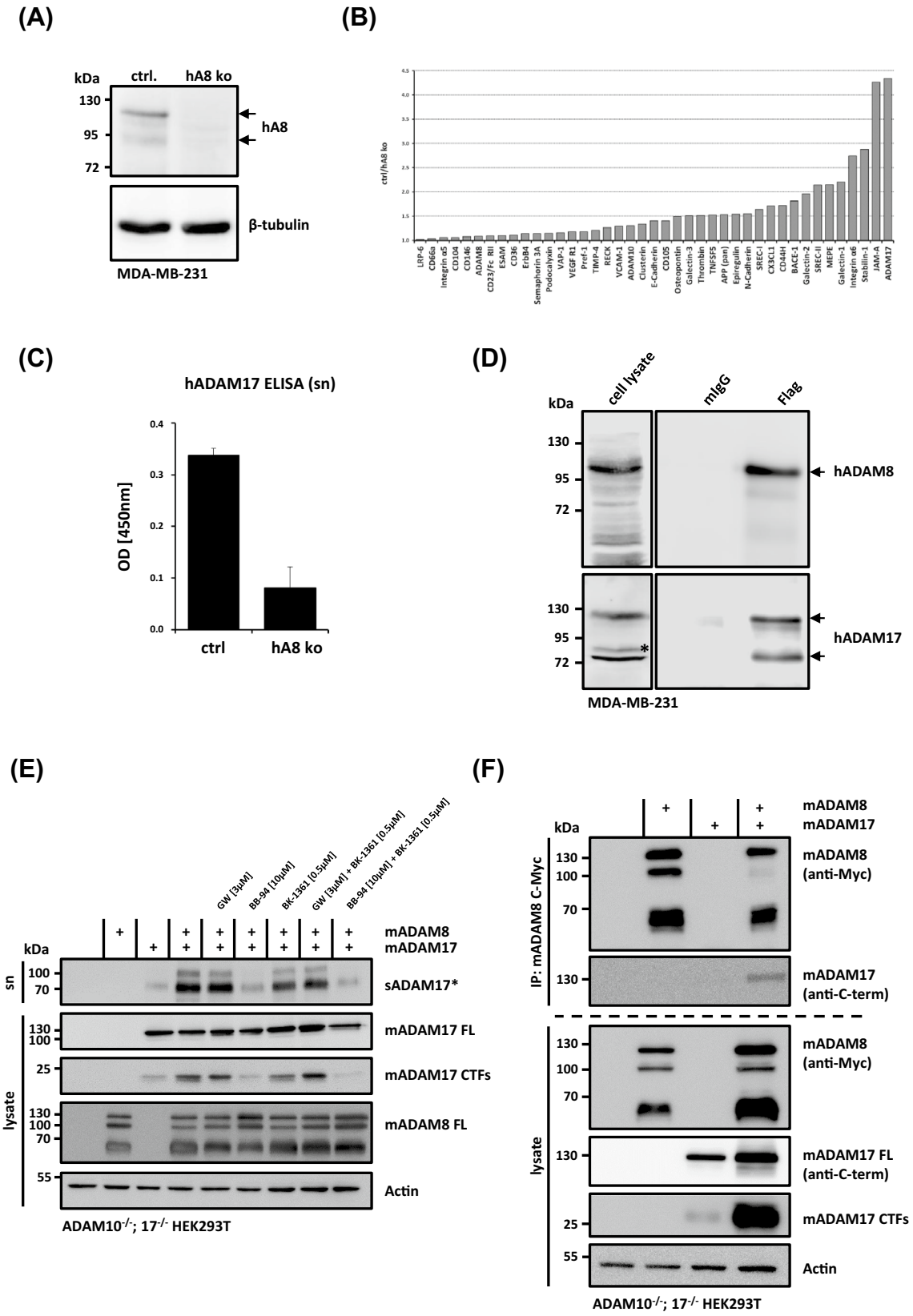

migration of MDA-MB-231 breast cancer cells. A knockdown of ADAM8 in this cell line caused a significant decrease in cell migration when compared to WT cells [33]. Based on this observation, an ADAM8-deficient MDA-MB-231 cell line was generated by CRISPR/Cas9 (Fig. 1a) and the release of other cell-surface receptors using a

commercial receptor array kit was analyzed (Fig. 1b). Interestingly, the amount of sADAM17 in the medium of MDA-MB-231 cells was significantly decreased in the absence of ADAM8, which was further confirmed by ELISA (Fig. 1c) with MDA-MB-231 cells, but also in another cancer cell line bearing an ADAM8 knockout (Fig. S1). Co-immunoprecipitation of ADAM8 and ADAM17 in transiently transfected MDA-MB-231 cells demonstrated a direct protein–protein interaction of ADAM17 and ADAM8 (Fig. 1d).

To investigate ADAM8-mediated ADAM17 shedding in more detail, ADAM10$^{-/-}$; 17$^{-/-}$ HEK293T cells were transiently transfected with murine ADAM17 and/or murine ADAM8 (Fig. 1e). Of note, ADAM17 shedding was already observed in ADAM17 single transfected cells but was largely increased in the presence of ADAM8, as indicated by the accumulation of ADAM17 C-terminal fragments (CTFs) in cell lysates and sADAM17 in the cell supernatants (Fig. 1e). qRT-PCR revealed endogenous expression of ADAM8 in ADAM10$^{-/-}$; 17$^{-/-}$ HEK293T cells, which might be responsible for the observed shedding of single transfected ADAM17 (Fig. S2). Application of the hydroxamate-based inhibitor GW280623 (GW), known to block ADAM17 activity [34], excluded an autocatalytic processing. For the inhibition of ADAM8-dependent ADAM17 shedding, the hydroxamate derivative Batimastat (BB-94) and the ADAM8 specific cyclic peptide inhibitor BK-1361 were used. Surprisingly, shedding of ADAM17 was only reduced in the presence of the membrane permeable BB-94 and not with BK-1361 (Fig. 1e). In a control experiment under the same conditions using CD23 as a well-described ADAM8 substrate, the inhibitory capacity of both inhibitors against ADAM8 was confirmed (Fig. S3A). Here the release of a ~ 36 kDa sCD23 form was decreased in the presence of BB-94 and BK-1361 as reported previously [35]. Notably, when analyzing cell supernatants an additional second fragment of sADAM17 appeared at ~ 100 kDa upon co-transfection with ADAM8. Using an N-terminal Strep-tagged ADAM17 it became apparent that this represents the pro-form of ADAM17 (Fig. S3B). Co-immunoprecipitation of mADAM8 and mADAM17 further supported close interaction of both murine proteases (Fig. 1f). Overall, the results indicate that ADAM8 can shed the pro- as well as the mature form of ADAM17.

Identification of sADAM10 and sADAM17 substrates by N-terminomics (TAILS)

Based on previous publications and our above described data, we assumed that shedding of ADAM10 and ADAM17 might be of particular importance in maintaining homeostasis of the cardiovascular system. Therefore, the murine cardiomyocyte cell line HL-1 was chosen for a mass spectrometry-based N-terminomics approach to identify possible substrates of soluble ADAM10/17. HL-1 cells are described to express ADAM10 and ADAM17 [36] and we could demonstrate by qRT-PCR that these cells additionally express ADAM9 and ADAM15 as sheddases for ADAM10 along with ADAM8 as sheddase for ADAM17 (Fig. S2).

For the N-terminomics TAILS approach, the ectodomains of the two target proteases ADAM10 and ADAM17 were expressed in insect cells and purified to homogeneity and validated by LC–MS/MS (Figs. 2a, S4). Activity measurements using specific fluorogenic peptides confirmed both proteases being proteolytically active. The selective inhibition of sADAM10 in the presence of the hydroxamate-based inhibitor GI254023X (GI) in comparison with the GW280623 (GW) inhibitor [34], blocking both ADAM10 and ADAM17, further confirmed the protease preparations as suitable for specific degradome studies (Fig. 2b). For the elucidation of specific cleavage events mediated by sADAM10 or sADAM17, the isolated secretome from HL-1 cells was incubated alone (non-treated control sample) or with the respective recombinant ADAMs for 16 h, in two technical replicates each, and subjected to a 6plex-TMT analysis (Fig. 2c). More than 95% of all peptide identifications (1078 unique peptides) carried an N-terminal TMT tag, indicating an original or a proteolytically generated protein N-terminus present prior tryptic digestion. We obtained TMT quantification values for 990 N-termini from 586 unique proteins. Determination of a TMT ratio cutoff to determine possible sADAM10/17 substrates was calculated according to a common TAILS protocol [37]. A > threefold change in sADAM10 or sADAM17-treated samples compared to the control was considered as a significant cleavage event for the respective protease.

Cleavage specificity of sADAM10 and sADAM17

From 968 quantified N-terminal peptides, 165 N-termini from 134 proteins displayed possible sADAM10 or sADAM17 cleavage events (Suppl. file 1). Only ratios that fulfilled the criteria for both replicates of sADAM treated replicates vs the averaged control signal were considered for the determination of the cleavage specificity and identification of potential substrates. Similar numbers of ADAM10 ($n = 42$) or ADAM17 ($n = 49$) specific events as well as a shared pool of cleavage events ($n = 45$) were identified (Fig. 2c). The revealed consensus sequences nicely fit to the previous studies, where cleavage preferences were assessed using peptide libraries as substrate [38, 39]. Overall, ADAM10 and ADAM17 showed comparable specificities for hydrophobic residues at P1′ position (Fig. 3a, b). While ADAM10 had a strong preference for leucine at P1′, ADAM17 additionally accepted the smaller residues valine

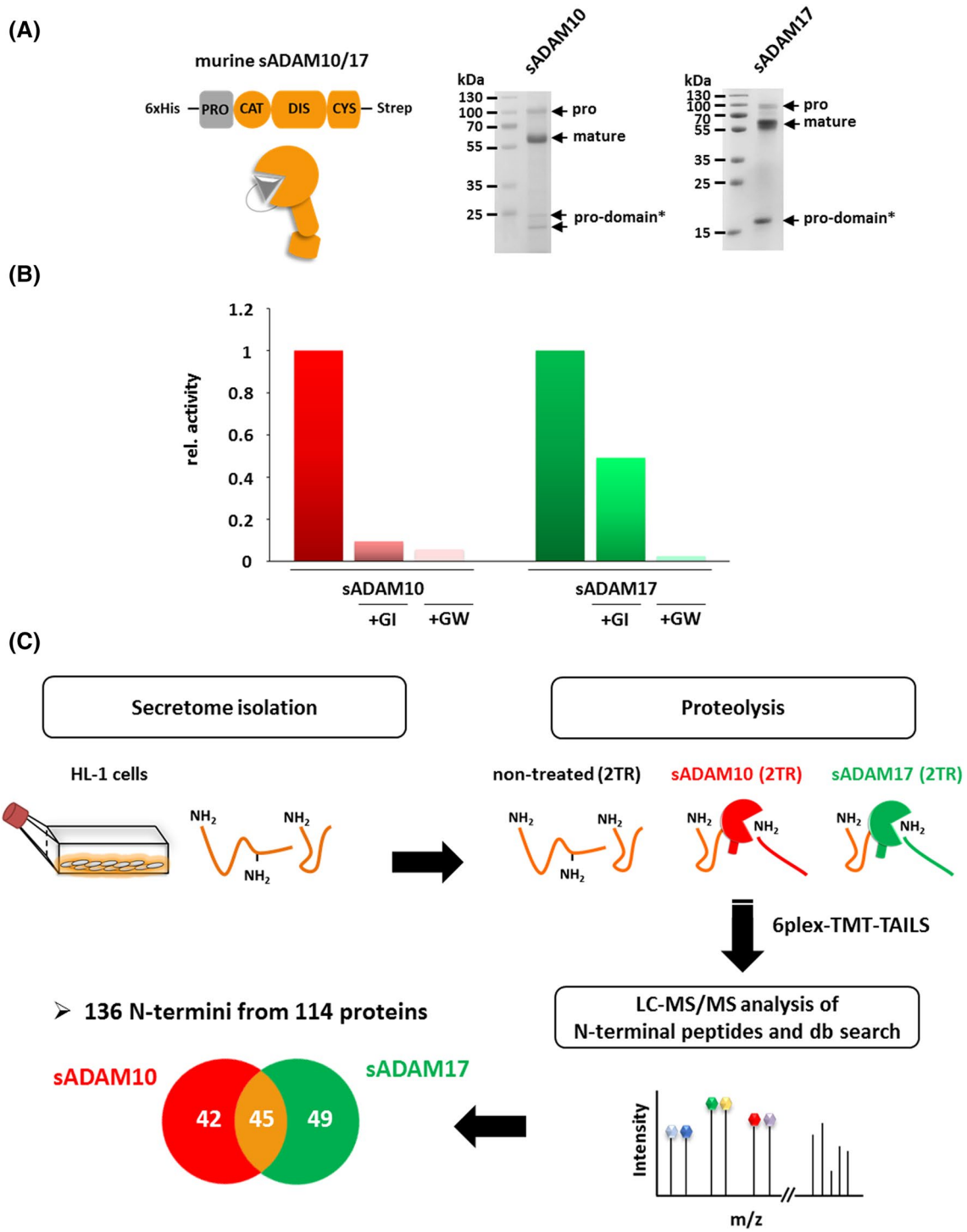

Fig. 2 Strategy for substrate screening of sADAM10 and sADAM17 employing the N-terminomics TAILS approach. **a** Domain structure of the recombinant murine sADAM10/17 constructs. The expressed and purified proteases comprise an N-terminal 6× His-tag followed by the prodomain (PRO), the disintegrin domain (DIS) and the cysteine-rich domain (CYS) with a C-terminal Strep-tag. Representative Coomassie-stained SDS-PAGE gels of 10 µg purified sADAM10 and sADAM17 are shown on the right. **b** Activity of purified recombinant sADAM10 and sADAM17 validated by a fluorogenic peptide-based cleavage assay. The proteases were inhibited by GI254023 (ADAM10) and GW280623 (ADAM10/17). **c** 6plex-TMT-TAILS workflow. Isolated HL-1 secretome treated with recombinant sADAM10 or sADAM17 was compared with untreated control samples. N-termini of the two internal technical replicates (TR) from each condition were labeled with TMT reagents 126–131. Following tryptic digestion, internal peptides were blocked and removed by a polyaldehyde dendritic polymer and N-termini (natural or TMT-labeled) were enriched for LC–MS/MS analysis. Venn diagram showing total numbers of identified proteins in both TR for sADAM10 and sADAM17 with a fold change > 3.0 compared to the control samples

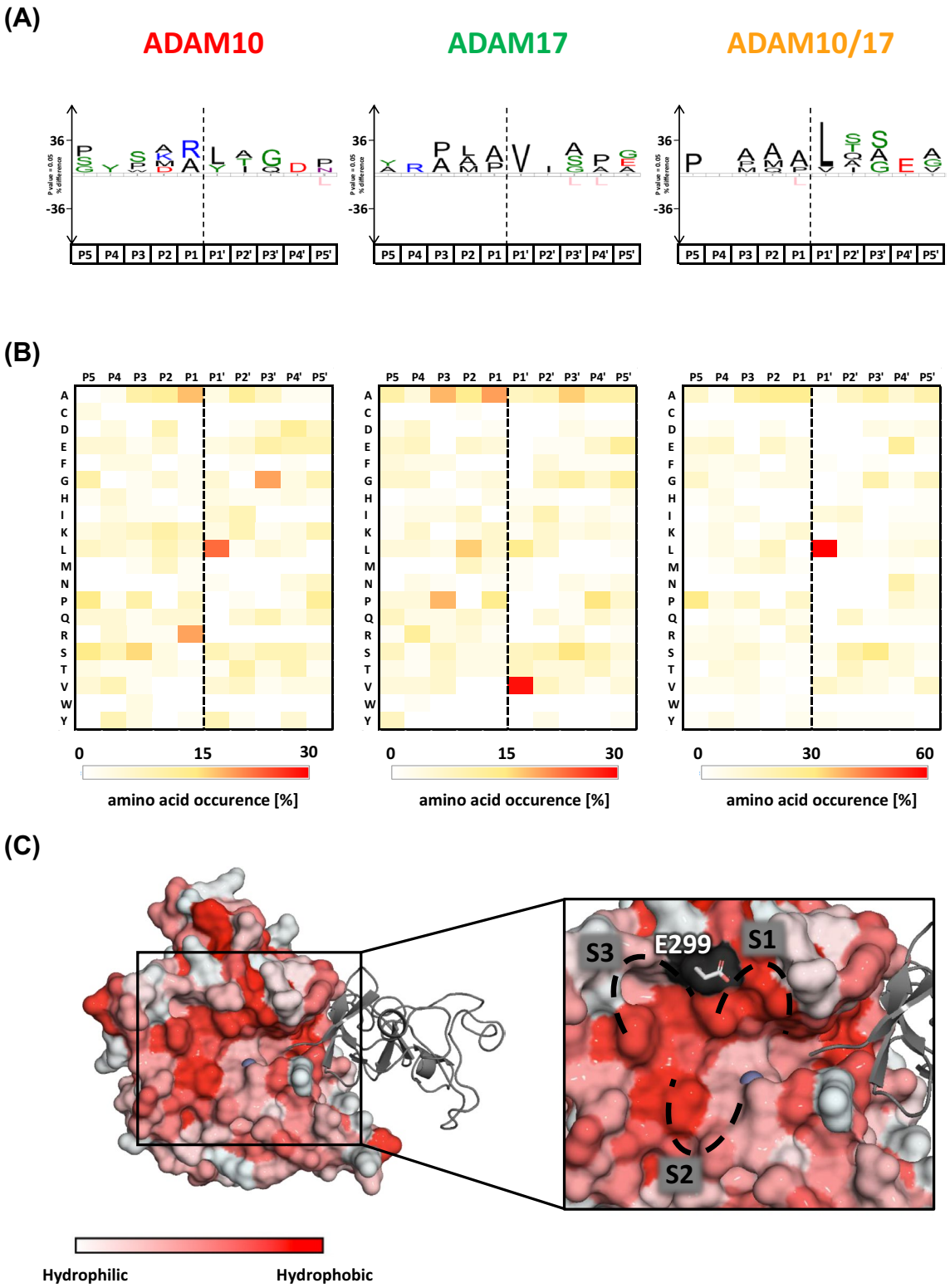

and alanine. Consistent with the previous reports was the quite loosely defined preference for aliphatic and neutral amino acids at P2′–P5′ and at P2–P5 (Fig. 3a, b). Notably, the preference for arginine at P1 observed for ADAM10 in the TAILS approach was much more pronounced compared to peptide substrates, indicative for the relevance of that position for protein binding and cleavage. Based on the crystal structure of the ectodomain of human ADAM10 [40], we propose that this arginine residue in a protein substrate might form a stabilizing salt-bridge with a glutamate residue

◂**Fig. 3** Cleavage specificity of sADAM10 and sADAM17 based on TAILS-identified substrates. **a** IceLogo and heat map, **b** analysis for amino acid occurrence in P5–P5′ of neo N-termini generated specifically by sADAM10 ($n=42$) and sADAM17 ($n=49$) and cleavage sites common for both proteases ($n=45$). Protein sequence logos were generated using iceLogo [94] with correlation for natural amino acid abundance in the mouse proteome, while heat maps show general percentage occurrence of amino acids within the data set. Dotted lines indicate cleavage sites. **c** P1 arginine preference of murine sADAM10. The homology model was generated based on the crystal structure of human ADAM10 (PDB: 6BE6). In the left panel the catalytic domain is shown as a molecular surface with a hydrophobicity sliding scale from white (polar) to red (hydrophobic), the cysteine-rich domain as a gray cartoon and the zinc ion as a light blue sphere. In the close up view (right panel) the substrate binding pockets S1–S3 are indicated with dashed lines. The suggested ADAM10 substrate stabilizing E299 residue is shown as sticks in a transparent surface pointing into the S1 pocket of the active site cleft

pointing into the S1 pocket of the active site (Fig. 3c). This particular glutamate residue seems to be a distinguishing feature for the active site of ADAM10, since in ADAM17, no corresponding acidic residue is present at the beginning of helix B (Fig. S5).

Validation of newly identified substrates of sADAM10 and sADAM17

Among the candidate substrates identified, we found 9 extracellular proteins with cleavage sites specific for either ADAM10 or ADAM17 as well as sites shared by both proteases (Table 1). Several of these proteins are representative candidates of the different components contributing to the defined structural and functional properties of the cardiac ECM [41], such as collagen IV and fibronectin as well as a non-structural matricellular protein thrombospondin-4 [42]. Furthermore, N-cadherin, a well-characterized cell adhesion molecule [43], cystatin C, a known protease inhibitor [44], and the hematopoietic macrophage colony-stimulating factor 1 (MCSF-1; [45, 46]) were identified as potential substrates for sADAM10/17.

To validate direct processing of selected candidate substrates by sADAM10 and sADAM17 in vitro, cleavage assays were performed and analyzed by SDS-PAGE and LC–MS/MS (Figs. 4, S6). In case of cystatin C, the TAILS analysis predicted an N-terminal cleavage event for sADAM17 between M29 ↓ L30. Indeed, a fragment of corresponding molecular weight could be detected upon digestion of murine cystatin C with recombinant sADAM17 and in solution LC–MS/MS confirmed the TAILS-derived cleavage site (Fig. 4a). Incubation of murine fibronectin with sADAM10 or sADAM17 resulted in multiple and distinct cleavage products for the two proteases, even though TAILS revealed only one newly generated N-terminus common for both enzymes (Fig. 4b). Due to the low sequence coverage (Fig. S6), it was not possible to identify the particular cleavage event at P1654 ↓ S1655 by MS. In case of N-cadherin, an already described shedding substrate of membrane-bound ADAM10 [47], the TAILS data likewise revealed one cleavage site between the extracellular domains two and three at position T386 ↓ F387 (Table 1) for sADAM10 and sADAM17. The in vitro incubation of a recombinant murine N-cadherin Fc chimera resulted in several low molecular weight fragments in the presence of sADAM10, including an N-terminal fragment of ~ 40 kDa consistent with the TAILS-identified cleavage sites (Fig. 4c). Conversely, using solely the N-cadherin ectodomain as substrate revealed further cleavage events, also in the presence of sADAM17 (Fig. S7). This was likewise reflected by the MS analysis (Suppl. File 2), which, amongst others, revealed an sADAM10/17 N-cadherin cleavage site one amino acid C-terminal to the site detected by TAILS. For PCPE-1, three specific neo N-termini generated by sADAM17 were identified within the CUB I domain (Table 1). The cleavage sites predict N- and C-terminal fragments of ~ 12 kDa and ~ 30 kDa, which is in accordance with the observed cleavage pattern (Fig. 4d). Indeed, all sites identified by the TAILS approach could be validated in in vitro cleavage assays analyzed by LC–MS (Suppl. file 2).The highest fold change in peptide abundance was observed for the position P118 ↓ V119. Therefore, we conclude that this cleavage corresponds to the two prominent protein fragments observed by SDS-PAGE (Fig. 4d).

Apart from all identified soluble protein substrates and intrigued by the observation that sADAM10 is able to process shed N-cadherin, we were interested to know whether other shedding substrate of membrane-bound ADAM10 and ADAM17 are also substrates of the soluble enzymes. To investigate this, the amyloid precursor protein APP was analyzed, which is an extensively studied ADAM substrate with regard to its function in Alzheimer's disease [48–50]. Incubation of the recombinant ectodomains of the two human APP isoforms 695 and 751 (additionally including a Kunitz-type protease inhibitor domain; KPI) with sADAM10/17 resulted in several distinct cleavage products (Figs. 5a, S8). LC–MS/MS analysis of these APP fragments was in line with our TAILS-identified cleavage specificity for ADAM10 and ADAM17 (Fig. 3a, b). Notably, two cleavage events in the stalk region of both APP isoforms at positions E590 ↓ I591 and E593 ↓ V594 (amino acid numbering corresponding to UniProt accession number P05067-4), suggested potential shedding sites different from the described α-secretase site K612 ↓ L613 within the Aβ peptide sequence [49].

Impact of N-terminal sADAM10/17 cleavage on cystatin C inhibition of meprin α

Since the N-terminus of cystatin C is known to be important for its inhibitory capacity, we examined the influence of the

Table 1 TAILS-identified sADAM10 and sADAM17 cleavage sites in native substrates

ECM protein	Protease	Cleavage site	TMT ratio[a] (protease/control)	
			ADAM10	ADAM17
PCPE-1	ADAM17	YDALE(95).(96)VFAGS	*(1.77)*	**9.50**
		GRFCG(112).(113)TFRPA	*(3.57)*	**10.90**
		FRPAP(118).(119)VVAPG	*(1.46)*	**5.42**
Fibronectin	ADAM10/17	VRWLP(1654).(1655)STSPV	**4.43**	**18.40**
Macrophage colony-stimulating factor 1 (CSF-1)	ADAM10/17	PSMAP(217).(281)LAGLA	**7.03**	**6.88**
Cadherin-2 (N-cadherin)	ADAM10/17	FTAMT(386).(387)FYGEV	**27.08**	**8.08**
Dickkopf-related protein 3 (Dickkopf-3; Dkk-3)	ADAM10/17	VFSET(131).(132)VITSV	*(3.03)*	**5.69**
Thrombospondin-4	ADAM10/17	QQSEP(212).(213)LAATS	**10.20**	*(2.50)*
	ADAM17	SEPLA(214).(215)ATSTG	*(1.86)*	**6.61**
Olfactomedin-like protein 2B (Photomedin-2)	ADAM10	HLRGR(288).(289)LASKP	**4.52**	*(1.85)*
Cystatin C	ADAM17	QGPRM(29).(30)LGAPE	*(2.13)*	**11.36**
		QGPRM(29).(30)LGAPE	*(1.17)*	**8.26**
Collagen alpha-2(IV) chain	ADAM17	GIPQK(1391).(1392)IAVQP	*(2.09)*	**4.69**

[a]TMT ratios are averaged values for both technical replicates vs average control values. TMT ratios in bold correspond to a fold change > 3 in both replicates, while values in italics and brackets do not fulfill all statistical selection criteria

observed truncation toward meprin α activity. In a previous study, it was shown that human cystatin C is an inhibitor of human meprin α [51]. Human and murine cystatin C share an overall sequence identity of ~ 71%, while especially, the N-terminal regions differ. Therefore, we also analyzed the processing of human cystatin C by murine sADAM10/17, to exclude possible species differences. Interestingly, the cleavage preference for human cystatin C was significantly shifted toward sADAM10 in comparison with the sADAM17 processed murine homolog (Fig. S9A). In case of human cystatin C, the sADAM10 cleavage was identified at position R34 ↓ L35 (Suppl. file 2), which is one amino acid N-terminal to the corresponding site in murine cystatin C (Fig. S9B). Finally, a fluorogenic peptide-based activity assay for human meprin α was employed, in which the protease activity was analyzed in the presence of full length or sADAM10/17 processed cystatin C proteins. Indeed, sADAM10/17 N-terminal truncated cystatin C resulted in decreased meprin α inhibition (Fig. S9C).

Shedding activity of sADAM10 and sADAM17

To elucidate whether the herein described proteolytic activity of sADAM10 and sADAM17 is restricted to soluble substrates and thus preventing shedding activity, we additionally analyzed the known membrane-bound targets APP [48, 52, 53] and the metalloprotease meprin β (Fig. 5b) [54–57].

As control, we co-transfected ADAM10$^{-/-}$; 17$^{-/-}$ HEK293T cells with either APP695 or APP751 and membrane-bound ADAM10 or ADAM17, respectively, which resulted in shed APP protein in the supernatant (Fig. 5b, c). As expected, investigating the shedding activity of the soluble proteases excluded sADAM10 as APP sheddase (Fig. 5b). Similar to that, no shedding of APP751 by sADAM17 was observed (Fig. 5c). However, in case of APP695, a low amount of soluble APPα (sAPPα) was detected in the cell-culture supernatants after incubation with recombinant sADAM17 (Fig. 5c). Shedding of APP695 by sADAM17 is further supported by an increase of APP CTFs in the cell lysates (Fig. 5c). Notably, only when sADAM17 was present, an additional higher migrating APP CTF signal appeared. The shift in size of the different CTFs is in agreement with the determined cleavage site from the LC–MS/MS analysis of the in solution digest of the soluble ectodomains (Figs. 5a, S8). As mentioned above, cleavage of APP by sADAM17 is further N-terminal to the previously identified α-secretase cleavage site at K612 ↓ L613 [49]. Using meprin β as known ADAM substrate, shedding was only observed in the presence of membrane-bound and not for soluble ADAM10 or ADAM17 (Fig. 5d). Overall, these results indicate in a proof of concept approach that sADAM17 still exhibits putative shedding activity toward a restricted panel of substrates (Fig. 5e).

sADAM10 and sADAM17 activities in the ECM

Employing the N-terminomics TAILS approach, we revealed a diverse degradome for sADAM10 and sADAM17 (Fig. 6). However, when analyzing candidate substrates of membrane-bound and soluble ADAM10 and ADAM17 using the

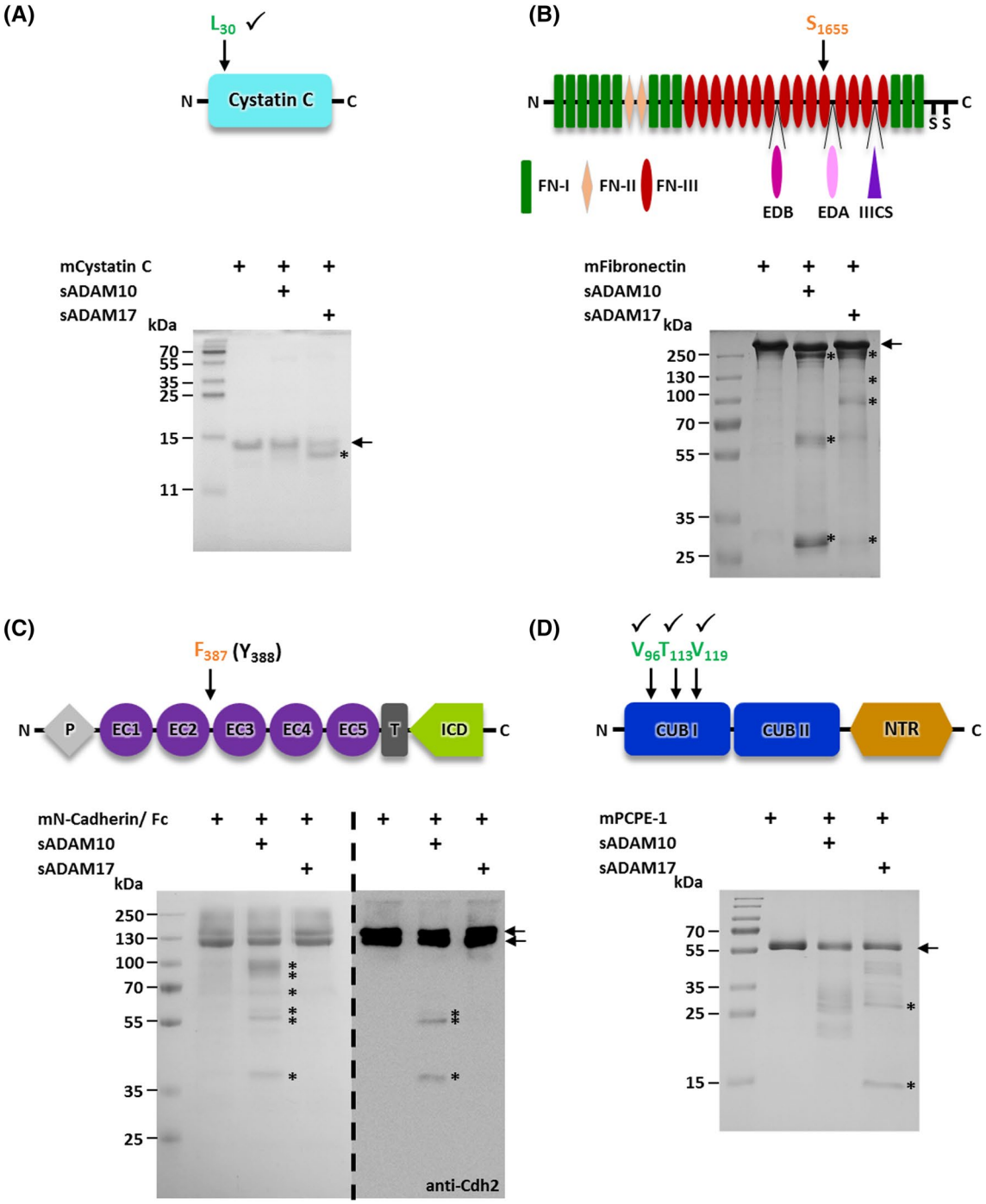

Fig. 4 Validation of TAILS-predicted substrates by in vitro cleavage assays and LC–MS/MS. Cleavage of recombinant proteins by sADAM10/17 was assessed by SDS-PAGE and visualized by Coomassie staining and immunoblotting. For each substrate the TAILS-predicted cleavage site(s) are highlighted by the P1′ position within the respective domain composition. Cleavage sites are colored according to specificity: green (sADAM17) and yellow (sADAM10/17). Proteolytic fragments generated by sADAM10 and/or ADAM17 are indicated by asterisks and full-length proteins by arrows. By LC–MS/MS confirmed cleavage events are marked with a tick. Processing of **a** murine cystatin C, **b** murine fibronectin and **d** murine PCPE-1 at a molar ratio of 10:1 with sADAM10 and sADAM17 or buffer alone. **c** In case of N-cadherin, the murine N-cadherin Fc chimera was incubated with sADAM10 and sADAM17 at a molar ration of 8:1 (left panel). Additional immunoblotting (right panel) using an N-terminal specific antibody confirmed the ~ 40 kDa cleavage fragment. *FN* fibronectin domain I–III, *EDB, EDA, IIICS* alternatively spliced regions, *P* prodomain, *EC* extracellular domain, *TM* transmembrane domain, *ICD* intracellular domain, *CUB* complement C1r/C1s, Uegf, Bmp1 domains I and II, *NTR* netrin-like domain

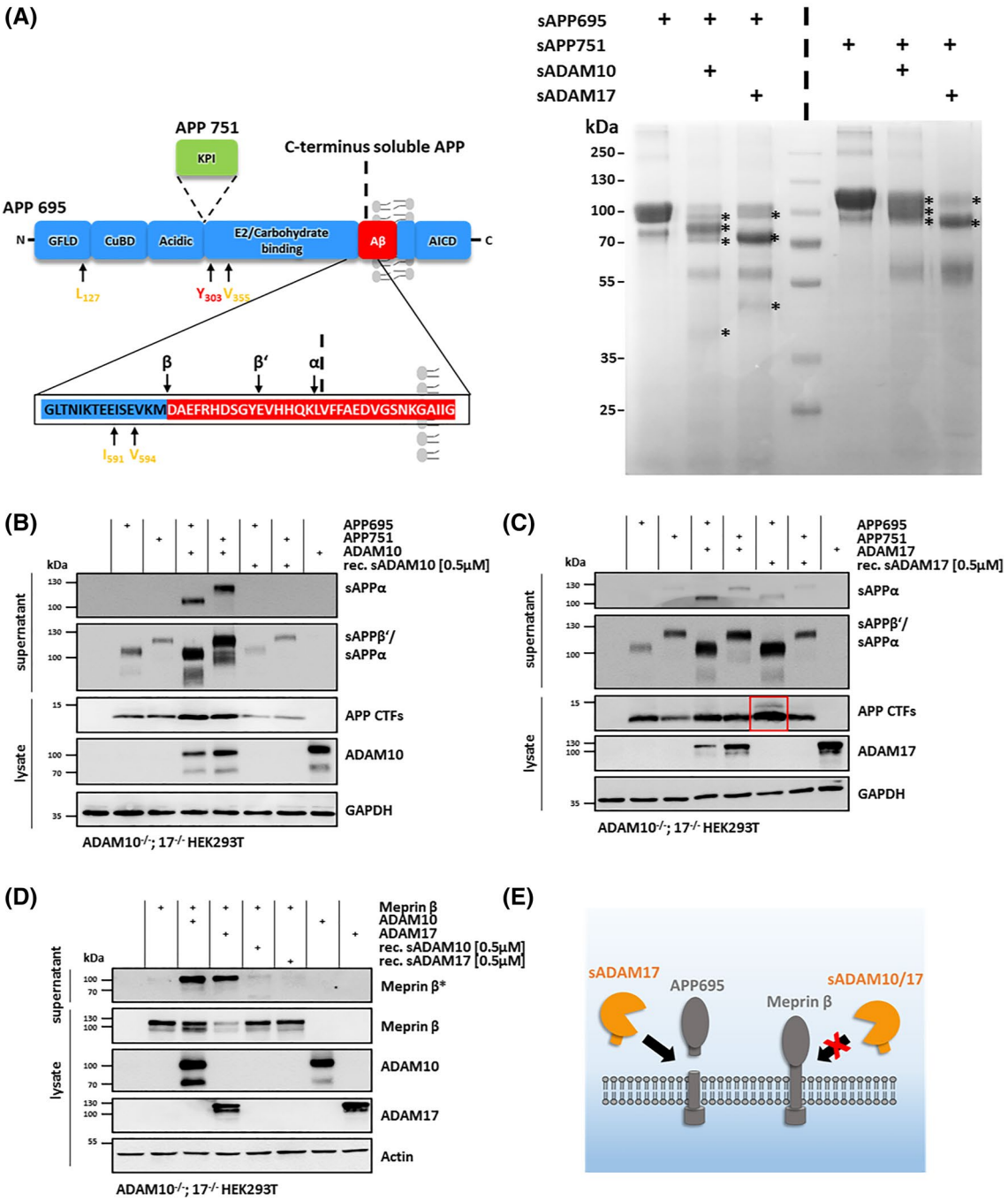

Fig. 5 Cleavage of APP and meprin β by sADAM10 and sADAM17. **a** Domain structure of APP with annotated α- and β-cleavage sites in the Aβ peptide region (left panel). Recombinant sAPP695 and sAPP751 were incubated in a molar ratio of 3:1 with sADAM10, sADAM17 or buffer alone. Cleavage products were separated by SDS-PAGE and visualized by Coomassie staining (right panel). Proteolytic fragments generated by sADAM10 and/or ADAM17 are indicated by asterisks. Selected high scoring PSM cleavage sites determined by LC–MS/MS are highlighted in the domain structure according to specificity: red (sADAM10) and yellow (sADAM10/17). GFLD: N-terminal growth factor-like domain, CuBD: copper-binding domain, KPI: kunitz protease inhibitor, E2: conserved region of the central APP domain, AICD: APP intracellular domain. **b–d** ADAM10$^{-/-}$; 17$^{-/-}$ HEK293T cells were either transfected with APP695, APP751 or meprin β alone or together with membrane-bound ADAM10 or ADAM17. In case of cells solely expressing APP695, APP751 or meprin β 0.5 µM recombinant sADAM10 or sADAM17 were added to the medium for 24 h before collecting the supernatants. Shedding of the target substrates was monitored by immunoblotting. **b**, **c** Shed APP was detected in the supernatants by immunoblotting using a sAPPα and sAPPβ′-detecting antibody (IC16) and a specific sAPPα antibody (14D6). Cells were additionally treated with DAPT to inhibit y-secretase and APP shedding was additionally monitored in the cell lysates using a C-terminal specific antibody (CT15). **d** Meprin β shedding was analyzed in ultracentrifuged supernatants (*) with an antibody raised against the ectodomain of meprin β. **e** Model of putative shedding activity of sADAM10 and sADAM17 summarizing the findings of experiments of **b–d**

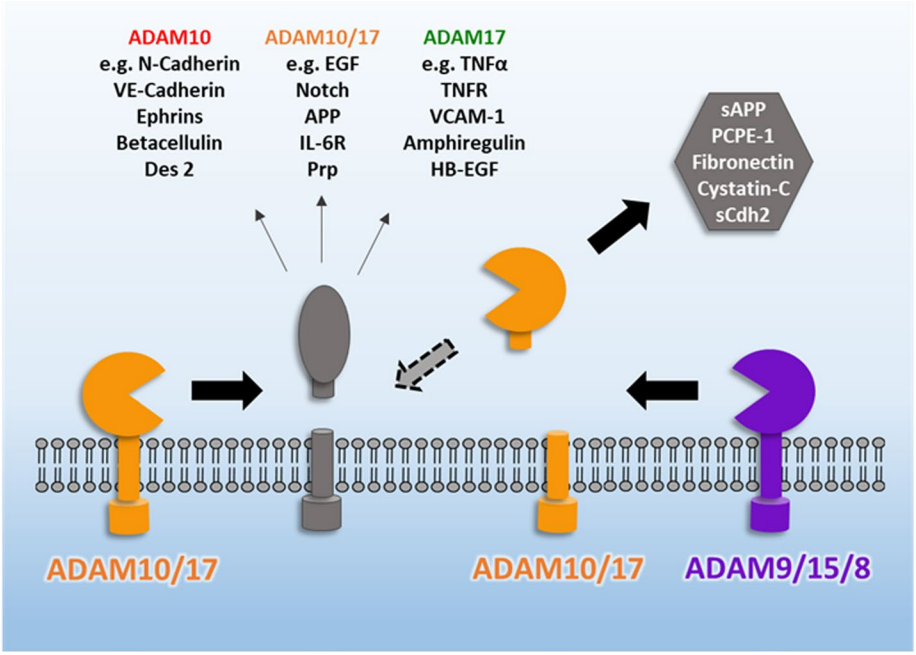

Fig. 6 Functional relevance of sADAM10 and sADAM17. Membrane-bound ADAM10 and ADAM17 are sheddases for a number of specific and common substrates. These seems to hold likewise true for sADAM10/17, even though the shed proteases have a different substrate pool like their membrane-bound counterparts

STRING database [58], a well-connected network between the different proteins was defined reflecting the complex nature of ECM homeostasis and remodeling (Fig. S10). The present study demonstrates once more the power of the TAILS approach for de novo substrate identification and provides a better understanding of the functional relevance of shed ADAM10 and ADAM17 within the protease web.

Discussion

Ectodomain shedding of membrane-bound proteins is an important regulatory event in many physiological and pathological conditions [1–4, 59]. Numerous in vivo and in vitro studies highlighted the particular importance of ADAM10 and ADAM17 for such proteolytic events [12, 13, 60]. However, what is only weakly addressed in this context is the turnover of active ADAM10 and ADAM17 at the cell surface. While internalization and exosomal release are under debate [29, 61–63], the consequences of proteolytic shedding of ADAM10 and ADAM17 by other proteases have not been investigated yet. For instance, shedding of ADAM10 by ADAM9 and ADAM15 has been described, but functional consequences have only been discussed with regard to impaired ectodomain shedding [28, 64]. For ADAM17, several studies report activity in plasma [30, 31], cerebrospinal fluid [65, 66], gingival crevicular fluid [67], and in kidney cyst fluids [68] without addressing the origin of the detected ADAM17 activity. With the identification of ADAM8 as a sheddase, we demonstrate for the first time that ADAM17 can indeed be proteolytically released from the cell surface. While classical ectodomain shedding occurs predominantly at the plasma membrane, our data suggest that ADAM8-mediated cleavage of ADAM17 partially happens on the secretory pathway. This notion is supported by the fact that full inhibition of ADAM8-dependent ADAM17 shedding was only achieved using BB-94, a hydroxamate inhibitor, which is membrane permeable in comparison with the cyclic peptide BK-1361. Encouraged by this and the fact that at least ADAM10 shedding is increased especially in the developing heart, we suggested the heart to be an interesting tissue and HL-1 cells to be an appropriate cell line to initially study the biochemical properties and functional relevance of sADAM10 and sADAM17 on secreted proteins.

N-terminomics TAILS has been demonstrated to be an efficient and straightforward technique for de novo substrate discovery [32]. Protein labeling with isobaric mass tags, e.g., TMT or iTRAQ reagents, allows simultaneous comparison of multiple samples and the quantification of protease-specific cleavage events. Employing a 6plex-TMT-TAILS approach, we present the first degradome study for sADAM10 and sADAM17. The analysis resulted in the identification of 136 sADAM10/17 cleaved N-termini from 114 proteins. The obtained cleavage specificity for a hydrophobic residue at position P1′ is in accordance with previous reports using peptide libraries [38, 39], which highlights the validity of the approach. A remarkable observation was the pronounced preference for an arginine residue at P1 for ADAM10, which is distinct to the previously published peptide-library-based PICS data [38]. While the protease domains of ADAM10 and ADAM17 resemble the characteristic fold of the adamalysin/ADAM family with an extended

zinc-binding motif and the conserved methionine turn, several insertion loops define unique surface features [40, 69]. The active site cleft is relatively flat on the non-prime side and becomes notched toward the prime side. Therefore, only subtle differences in the groove width of the binding pockets, especially the one of the S1′ pocket, define substrate specificity of ADAM10 and ADAM17 as reflected by the determined cleavage specificity. The S1 pocket itself is quite small, which is consistent with the preference for alanine at P1 for both proteases in general. Considering that native substrates have a complex fold in comparison with rather short peptides, additional interactions regulate substrate binding. Therefore, it is likely that the glutamate residue protruding into the S1 pocket in ADAM10 stabilizes substrates via a salt bridge over an arginine residue at the P1 position. Nonetheless, deduced from known ADAM10 shedding sites as well as from the herein identified cleavage sites in ECM substrates, it is also evident that this preference is not a prerequisite for substrate cleavage. Overall, we conclude that not only membrane-bound ADAM10 and ADAM17, but also their shed forms need a tight spatial and temporal regulation to ensure selective substrate specificity in vivo. One such regulation can be achieved by tissue inhibitors of metalloproteinases (TIMPs), which are endogenous inhibitors of matrix metalloproteinases (MMPs) and ADAMs [70]. TIMP-3 inhibits ADAM10 and ADAM17 [71, 72], whereas ADAM10 is additionally targeted by TIMP-1 [71]. Interestingly, particularly in hearts of patients with dilated cardiomyopathy, TIMP-3 levels are decreased, while ADAM15, ADAM10, and ADAM17 expression is elevated [24]. This suggests a less stringent proteolytic control of membrane-bound and soluble ADAM10/17 during the progress of the disease. However, it is possible that sADAM10/17 have an additional non-proteolytic regulatory function in complexing TIMPs in the ECM and serum, thereby down-regulating their inhibitory capacity also toward other target proteases. Nonetheless, the proposed physiological mechanisms have to be proven in further studies in vivo.

Besides the well-characterized sheddome of ADAM10 and ADAM17, the TAILS approach led to the identification of unique and common substrates for sADAM10 and sADAM17. Initial candidate substrate validation by in vitro cleavage assays and in solution LC–MS/MS further confirmed these findings. For example, fibronectin and sN-cadherin are directly processed by both ADAM10 and ADAM17, whereas cystatin C and PCPE-1 are preferred substrates of sADAM17 only. Apart from the TAILS analysis, the ectodomains of APP695 and APP751 are cleaved by both proteases specifically and at common sites. Although the in vitro cleavage specificities are in general accordance with the TAILS-identified N-termini, some discrepancies were observed, which could have different reasons. For example, alternative cleavage sites were not detectable by mass spectrometry due to technical issues, such as peptide length or inefficient ionization [73]. Another explanation is that in vitro assays are limited in recapitulating the complexity of a secretome sample. Hence, detection of indirect or secondary cleavage events of the analyzed target protease, a hallmark of the protease web, is difficult [74]. Interactions of a substrate with other proteins may result in structural conformational changes that are prerequisite for the protease accessibility to the cleavage site. Our data on murine vs human cystatin C cleavage by sADAM10/17, furthermore, show that already subtle differences in sequence can have an impact on substrate specificity of the two proteases. However, since the cystatin C inhibition mechanisms vary depending on the target protease, it needs to be proven whether the described N-truncation by sADAM10/17 is of physiological relevance. Especially in the context of heart remodeling and/or heart diseases, there are so far no reports about N-terminal truncated cystatin C variants.

The TAILS data and the biochemical analysis of substrates clearly demonstrate proteolytic activity of shed ADAM10 and ADAM17. Hence, we investigated if this activity is strictly restricted to soluble substrates. For instance, membrane-bound activated meprin β can act as sheddase for several proteins such as APP [75] or the IL-6R [76]. Soluble meprin β has no shedding activity toward these substrates, but cleaves, e.g., APP within the N-terminal region, generating non-toxic APP fragments [59, 75] or mucine 2 in the intestine [77]. Prototypically, meprin β itself as well as the two APP variants APP695 and APP751 were used as substrates to investigate potential shedding by sADAM10/17 in cellulo. Our data suggest that membrane tethering of ADAM10/17 is of general importance for their shedding activity and efficiency, most likely to enable close proximity to the stalk regions of the substrates and concomitantly the association to the activity regulating iRhoms [78, 79]. Therefore, the observed shedding of APP695 in the presence of sADAM17 might be due to the unphysiological high concentrations of the protease. However, these data demonstrate the general possibility of persistent shedding activity for soluble ADAM17 which should be considered with regard to the overall debate on major determinants of shedding activity [1].

In sum, the TAILS N-terminomics data together with the shedding activity assays provide proof of concept that sADAM10 and sADAM17 may exhibit additional biological roles within the protease web (Figs. 6, S10). Therefore, the identified unique and overlapping substrates pave the way for further studies to understand the physiological relevance of the sADAM10 and sADAM17 degradome in health and disease.

Experimental procedures

Chemicals

All chemicals were of analytical grade and obtained from Carl Roth GmbH + Co. KG, Merck KGaA, Sigma-Aldrich Inc. and Thermo Fisher Scientific Inc., if not stated otherwise.

Cells

The murine HL-1 cells were generously provided by William C. Claycomb (Department of Biochemistry and Molecular Biology, Louisiana State University Health Sciences Center, New Orleans, Louisiana). The cells were cultured in Claycomb media (Sigma-Aldrich Inc.) supplemented with 10% (v/v) fetal calf serum (FCS), 2 mM L-glutamine, 0.1 mM norepinephrine in ascorbic acid, 100 units/l penicillin, and 100 µg/ml streptomycin at 37 °C in a 5% CO_2 atmosphere.

ADAM10$^{-/-}$; 17$^{-/-}$ HEK293T [80] were maintained in Dulbecco's modified eagle medium (DMEM; Gibco™) with GlutaMAX™ supplemented with 10% (v/v) FCS, 100 units/l penicillin and 100 µg/ml streptomycin under humidified conditions (5% CO_2) at 37 °C.

The CRISPR/Cas9 knockout/knockin kit from OriGene (# KN213386) was used to generate a genomic ADAM8 knockout in MDA-MB-213 and AsPC1 cells. In brief, the pCas-Guide vector with the ADAM8 target sequence (gRNA) near to the 5′ end of the ADAM8 ORF or a scramble gRNA control was transfected together with a knockin vector into both cell lines using lipofectamine LTX (Invitrogen AG). The knockin vector contains between the left and right ADAM8 homology arms a functional GFP and puromycin cassette. After homology recombination, the GFP is under the control of the native ADAM8 promoter and the puromycin gene is under a PGK promoter. The transfected cells were split several times in the following 3 weeks before starting the selection with 5 µg/ml puromycin (InvivoGen) to get single-cell clones. MDA-MB-231 were cultured in DMEM (Biochrome GmbH) and AsPC1 in RPMI (Biochrome GmbH) with GlutaMAX™ supplemented with 10% (v/v) FCS (Biochrome GmbH).

ELISA

MDA-MB-231 and AsPC1 cell clones were incubated for 16 h at 37 °C in growth medium. A soluble human ADAM17 (# DY930) enzyme-linked immunosorbent assay (ELISA; R&D Systems Inc.) was used to detect soluble ADAM17 in cell-culture supernatants.

Soluble receptor array

Relative levels of 119 soluble receptors and related proteins secreted into the medium of MDA-MB-231 control and ADAM8 knockout clones was assessed using the Proteome Profiler™ Human Soluble Receptor antibody array (Non-hematopoietic Panel, R&D Systems, # ARY012). Briefly, 5×10^5 cells were cultured for 48 h in serum-free DMEM medium. The conditioned medium was centrifuged at 15,000×*g* for 15 min to remove cell debris and subjected to the antibody array according to the manufacturer's protocol. The signal intensity of the detected proteins was measured using ImageJ (NIH, Bethesda, MD, USA).

RNA extraction and cDNA synthesis

Total RNA was extracted from HL-1 and ADAM10$^{-/-}$; 17$^{-/-}$ HEK293T cells using the NucleoSpin®RNA Isolation Kit (MACHEREY–NAGEL GmbH & Co. KG). The concentration, purity, and integrity of the isolated RNA were determined by a NanoDrop™ 2000 instrument (Thermo Fisher Scientific Inc.). One microgram of RNA was used as input for complementary DNA (cDNA) synthesis using the RevertAid First Strand cDNA Synthesis Kit (Thermo Fisher Scientific Inc.), according to the manufacturer's instructions.

Quantitative real-time PCR analysis

Quantitative real-time PCR (qRT-PCR) assays were performed based on the hydrolysis probe technology on a LightCycler® 480 instrument (Roche Deutschland Holding GmbH) using the 2× LightCycler® 480 Probes mastermix (Roche Deutschland Holding GmbH). For primers and UPL probes, see Suppl. Table S1. Primers were purchased from Sigma-Aldrich Inc. The qRT-PCR was performed in three technical replicates on each sample for each gene tested. Cycling conditions were as follows: 10 min at 95 °C, followed by 45 cycles each consisting of 10 s at 95 °C and 30 s at 60 °C, and a cooling step of 30 s at 40 °C (ramp rate of 4.8 °C/s). The crossing point (Cp) data were analyzed using the absolute quantitation algorithm for each sample. Delta Cp was calculated by subtracting the GAPDH control gene Cp from Cp of the test gene.

Recombinant sADAM10 and sADAM17

The ectodomains of murine ADAM10 (UniProt accession number: O35598, amino acid residues 20-673) and ADAM17 (UniProt accession number: Q9Z0F8, amino acid residues 18-671) were amplified from respective full-length cDNA and cloned into pFastBac (Gibco™) containing a meprin β signal peptide [81], followed by an N-terminal 6× His-tag and a C-terminal Strep-tag. Sigma-Aldrich

Inc. synthesized primers and sequences of the constructs were verified by DNA sequencing (GATC Biotech AG). Expression and purification were performed as previously described [38]. The purity of the enzyme preparations, in particular the absence of other proteases, was confirmed by LC–ESI MS (data are deposited at the server ProteomeXchange). Therefore, 20 µg of sADAM10 and sADAM17 were dissolved in 2 M Urea in 100 HEPES buffer (pH 8.0). Samples were reduced with dithiothreitol (5 mM) for 1 h at 37 °C and alkylated with iodoacetamide (12.5 mM) for 1 h at 25 °C. Samples were split into two and either incubated with or without 500 units of PNGaseF (New England Biolabs GmbH) overnight at 37 °C. Samples were further split into two and left to be digested overnight at 37 °C with either 100 ng of trypsin (10 mM ABC, 25 mM HEPES buffer) or 100 ng of chymotrypsin (25 mM HEPES, pH 8.0, 1 mM $CaCl_2$). Samples were diluted with 1% FA and analyzed by LC–MS. Samples were analyzed on a Thermo Q-Exactive Plus mass spectrometer (Thermo Fisher Scientific Inc.). The samples were concentrated and washed for 4 min (Acclaim Pepmap 100 C18, 5 mm × 300 µm, 5 µm, 100 Å, Dionex) with 3% ACN/0.1% TFA at a flow rate of 30 µl/min prior to peptide separation using an Acclaim PepMap 100 C18 analytical column (50 cm × 75 µm, 2 µm, 100 Å, Dionex). A flow rate of 300 nl/min using eluent A (0.05% FA) and eluent B (80% ACN/0.04% FA) was used. Peptides were separated over 40 min by increasing the concentration of eluent B from 5 to 50%. The column was subsequently washed by increasing eluent B to 95% over 1 min, and after a further 10 min at 95% B, the system was equilibrated at 5% B for 15 min. The ten most intense precursors with charge states greater than 2+ were selected for HCD fragmentation using a normalized collision energy of 25 at a resolution of 17,500.

Fluorogenic peptide-based activity assay

The enzymatic activity of sADAM10 or sADAM17 was analyzed using the quenched fluorogenic peptide substrates Acetyl-dArg(3)-dGlu(3)-hexaminoyl-K(Dabcyl)-PRYEAYKMGK(5FAM)-C-NH2 (BioZyme Inc.) for sADAM10 and Mca-PLAQAV(Dpa)RSSSR-NH_2 (R&D Systems) for sADAM17 at final concentrations of 10 µM. For inhibition studies, GI254023 (ADAM10) or GW280623 (ADAM10 and ADAM17) (Iris Biotech GmbH) were added to final concentrations of 3 µM. For murine and human cystatin C inhibition studies, the activity of 1 nM recombinant meprin α was monitored using a specific quenched fluorogenic peptide Mca-HVANDPIW-dnp (Genosphere Biotechnologies) [82]. Recombinant meprin α was expressed and purified as described previously [83]. For inhibition analysis, meprin α was incubated with 1 µM full-length or sADAM10/17 processed (ratio 1:10 sADAM10/17 to cystatin C, 16 h, 37 °C) cystatin C for 30 min at 37 °C. As control, the activity of the same amount of sADAM10/17 toward the fluorogenic substrate was determined. Immediately before measurement 10 µM of the quenched fluorogenic peptide, substrate was added. All activity assays were carried out in 20 mM HEPES buffer (pH 7.5) in duplicates at 37 °C. Proteolytic activity was measured as relative fluorescence units (RFU) every 30 s for 120 min, at excitation 405 nm and emission 320 nm, using the Tecan Infinite® F200 PRO plate reader (Tecan Trading AG). The activity was determined from the slope of the linear range of the curve normalized to the initial point of the measurement and presented as bar graph.

TAILS

For proteomic analysis, murine HL-1 cells were grown to ~ 70% confluency. Cells were then intensively washed with PBS (Gibco™) and grown in DMEM medium without serum and phenol red. After 48 h, the conditioned medium was collected and protease inhibitor cocktail (cOmplete™, Roche Deutschland Holding GmbH) immediately added. Cell debris was removed by centrifugation (5 min, 2200×*g*) and filtration (0.22 µM). The secretome was concentrated at 4 °C by ultrafiltration using Amicon Ultra-15 centrifugal filter units (10 kDa cutoff, Merck Millipore Ltd.). Within the same concentrating device, the buffer was exchanged to 100 mM HEPES (pH 7.0) by five cycles of dilution and concentration. A protein concentration of 2.4 mg/ml was determined using the BCA protein assay kit (Thermo Fisher Scientific Inc.). The secretome preparation was aliquoted, snap frozen in liquid nitrogen, and stored at − 80 °C until further use.

Equal amounts of concentrated secretome were incubated for 16 h at 37 °C with recombinant sADAM10 or sADAM17 in a ratio of 1:100 protease to secretome, as previously described for matrix metalloproteinases (MMPs) [84]. Non-treated control samples received an equivalent of buffer only. All individual experiments were performed from secretome aliquots of the same batch and in two technical replicates each.

The TAILS analysis followed the previously published protocol [32], but used 6plex-TMT reagents (Thermo Fisher Scientific Inc.). From each reduced and alkylated sample, 0.2 mg of proteins were labeled using 1.6 mg TMT reagent per channel in 50% DMSO (final concentration) for 30 min at room temperature. The reaction was quenched with 100 mM ammonium bicarbonate for 15 min and the samples were combined. The following steps of tryptic digestion and enrichment of N-terminal blocked peptides were carried out according to Kleifeld et al. [32].

LC–MS/MS analysis was performed using a Dionex U3000 nanoHPLC coupled to a Q-Exactive Orbitrap mass spectrometer (both from Thermo Fisher Scientific Inc.). In

two technical replicates, 5 µl of TAILS enriched and TMT-labeled peptides were injected and loaded on a trap column (Acclaim Pepmap 100 C18, 10 mm × 300 µm, 3 µm, 100 Å, Dionex). Trapping was performed for 3 min with 3% ACN/0.1% TFA at a flow rate of 30 µl/min. Peptide separation was performed using an Acclaim PepMap 100 C18 analytical column (15 cm × 75 µm, 3 µm, 100 Å, Dionex) with a flow rate of 300 nl/min. Peptides were separated using a linear gradient from 5 to 50% B (solvent A: 0.04% formic acid; solvent B: 80% acetonitrile/0.04% formic acid) in 180 min followed by 40–95% B in 5 min, 95% B for 10 min and equilibrating at 5% B for 11 min. Ionization was performed with 1.5 kV spray voltage applied on a liquid junction emitter (10 µm tip size, New Objective, Woburn, MA, USA) with the source temperature set to 250 °C. MS data were acquired from 5 to 205 min with MS full scans between 300 and 1800 *m/z* at a resolution of 60,000 at *m/z* 400. The 15 most intense precursors with charge states ≥ 2+ were subjected to fragmentation with HCD with NCE of 32.5; isolation width of 2 *m/z*. Dynamic exclusion for 90 s was applied with a precursor mass tolerance of 5 ppm. Lock mass correction was performed based on the polysiloxane contaminant signal of 445.120025 *m/z*.

The acquired MS/MS spectra from two technical replicates were searched using SequestHT within Proteome Discoverer 1.4 (Thermo Fisher Scientific Inc.) against the entire reviewed database of *Mus musculus* (Ensembl 86) with known proteoforms and common contaminants (24,754 sequences). Modifications for the database search were static carbamidomethylation on cysteine residues, dynamic oxidation on methionine residues, static TMT-6plex on lysines, and dynamic TMT-6plex on the peptide N-terminus. Spectra were searched with semi-tryptic enzyme specificity. MS mass tolerance was set to 5 ppm and MS/MS tolerance was set to 0.04 Da. A decoy search determined false-discovery rate of 1% was applied using the Percolator algorithm. TMT reporter ion intensities were extracted and missing reporter ions replaced by minimal values. sADAM10/17 to control and ADAM10 to ADAM17 ratios for both technical replicates were calculated using Proteome Discoverer 1.4 software package.

Determination of a TMT ratio cutoff to determine possible ADAM10/17 substrates was calculated according to a common TAILS protocol [37]. In short, five times the standard deviation (SD) from the normal distribution of control 1 vs control 2 ratios indicated a stringent protease treated vs control ratio cutoff, which corresponded to a fold change between control and sADAM10/17-treated sample of > 3. Furthermore, to ensure reproducibility between protease-treated technical replicates and to remove outliers, only ratios of ADAM-treated replicates 1 and 2 vs the averaged control that fulfilled the criteria for both replicates were considered to indicate a potential substrate for the respective protease.

Substrate cleavage assays

Recombinant sADAM10 or sADAM17 were incubated with candidate substrates in 20 mM HEPES pH 7.5 for 16 h at 37 °C. Recombinant human APP695 and APP751 were expressed and purified as described previously [75, 85]. Other proteins were purchased as follows: murine cystatin C (# RD272009025; BioVendor-Laboratorni medicina a.s.), human cystatin C (# RD172009; BioVendor-Laboratorni medicina a.s.), mouse N-cadherin Fc chimera (# 6626-NC; R&D Systems), mouse N-cadherin (# 50752-mcch, Sino Biological Inc.), mouse PCPE-1 (# 2239-PE-020; R&D Systems Inc.), and mouse fibronectin (# ab92784; Abcam plc.). For cleavage site determination, 10 µg of human APP695 and APP751 were incubated with sADAM10 or sADAM17 in a 3:1 ratio. 4 µg of the N-cadherin proteins were processed at a substrate to protease ratio of 8:1. For murine and human cystatin C (4 µg), PCPE-1 (5 µg), and fibronectin (15 µg), a ratio of the respective substrate to sADAM10 and/or sADAM17 of 10:1 was chosen. Reaction products were analyzed by SDS-PAGE and visualized by Coomassie staining or immunoblotting as well as by LC–MS/MS.

LC–MS/MS analysis of in vitro substrate cleavage by sADAM10/17

For cleavage site determination, digested proteins and undigested controls of the substrate cleavage assays were denatured and unfolded by the addition of 2 M guanidine hydrochloride followed by heating the sample to 60 °C for 20 min. 10 mM of DTT was added and the samples incubated at 60 °C for 30 min. Alkylation of cysteine residues was achieved by adding 55 mM iodoacetamide and incubation for 1 h at RT in the dark. Reductive dimethylation of primary amine groups was carried out by the addition of 30 mM formaldehyde and 30 mM of sodium cyanoborohydride. Samples were incubated over night at 37 °C and the reaction was quenched by the addition of 100 mM ammonium bicarbonate. Subsequently, the samples were acidified using 10% formic acid and lyophilized in a speedvac. Proteins were redissolved in ^{18}O-water to decrease the guanidinium hydrochloride concentration to 0.5 M and the pH was adjusted to 7.5. For the cleavage analysis of human APP695, APP751, human cystatin C, and the mouse N-cadherin Fc chimera, the samples were then digested using trypsin or chymotrypsin (100 ng protease per sample) at 37 °C overnight. In case of murine cystatin C, murine fibronectin, murine PCPE-1, and murine N-cadherin, one aliquot was digested using LysC/trypsin and another one using chymotrypsin. The respective endoprotease (1:50) was added and the samples were

digested over night at 37 °C. All samples were acidified with 10% formic acid. Trypsin and chymotrypsin or LysC/trypsin and chymotrypsin treated identical samples were combined and peptides were purified using the C18 Sep Pak column system. Elution of peptides was achieved using sequential elution using 50% and 100% ACN. Samples were lyophilized and reconstituted in 5% formic acid prior to LC–MS analysis on an Orbitap-Velos mass spectrometer (Thermo Fisher Scientific Inc.). The mouse N-cadherin Fc chimera sample was measured on an Orbitrap Q-Exactive mass spectrometer (Thermo Fisher Scientific Inc.).

The acquired MS/MS spectra were searched with SequestHT against the *Homo sapiens* (49,429 entries) or *Mus musculus* (17,453 entries) database using Proteome Discoverer 1.4 containing the proteins of interest as well as common contaminants. Static modifications applied for searches were carbamidomethylation on cysteines. Dimethylation of lysines and peptide N-termini, oxidation on methionines and ^{18}O C-terminal labeling were set as variable modifications. Spectra were searched with semi-enzyme specificity for trypsin and full enzyme specificity for chymotrypsin. An MS mass tolerance of 10 ppm and an MS/MS tolerance of 0.04 Da were used.

Peptide grouping was applied to group peptides spectrum matches (PSMs) with the same modification under the same peptide. Peptides were identified using a false-discovery rate ≤ 0.01 (high). Ion intensities, as well as peptide spectral match counts, for all identified peptides were extracted from the data and N-terminally dimethylated as well as peptides lacking the C-terminal ^{18}O label were considered to indicate a possible sADAM10 or sADAM17 prime or non-prime cleavage site if they displayed a strongly higher abundance in the sADAM10/17-treated samples (> eightfold change, Suppl. file 2).

Shedding assay

For shedding experiments, ADAM10$^{-/-}$; 17$^{-/-}$ HEK293T cells were used, kindly provided by Dr. Björn Rabe, University of Kiel. Transient transfection was performed at 80–90% cell confluence with the following constructs: pcDNA3.1 (empty vector), murine ADAM10 and murine ADAM17 in pcDNA3.1, double tagged murine ADAM17 in pcDNA 4/TO, murine ADAM8 in pCMV6, human ADAM8 in pAAVS1, human CD23 in pIRES2-EGFP, human meprin β in pSG5, human APP695 and APP751 in pCIneo. For transfection, plasmids were mixed with the transfection reagent polyethyleneimine (PEI, Polysciences Europe GmbH) in a ratio of 1:3 in serum-free medium. After an incubation step of 30 min at room temperature, the mixture was added to the cells for 5 h and then replaced by fresh medium. After 24 h of serum starvation, culture medium was replaced with fresh serum-free medium alone or containing 0.5 µM recombinant sADAM10 or sADAM17. For the detection of C-terminal fragments (CTFs), the medium was additionally supplemented with the γ-secretase inhibitor DAPT. After 24 h, cell-culture supernatants were collected, cleared by centrifugation (15,000×*g*, 5 min, 4 °C) and cells harvested. For the analysis of ADAM17, CD23 and meprin β shedding cell supernatants were additionally ultracentrifuged at 186,000×*g* for 2 h at 4 °C. For a comparable analysis of possible shedding events, supernatants were normalized to the protein content of the respective cell lysates and analyzed by immunoblotting. For concentration of respective supernatant, proteins were precipitated with trichloracetic acid [TCA 10% (wt/vol)]. After incubation on ice for 60 min, proteins were pelleted (15,000×*g*, 15 min, 4 °C), washed with acetone, and dissolved in SDS-PAGE loading buffer.

Co-immunoprecipitation

The MDA-MB-231 ADAM8 knockout cell clone was transiently transfected with a human ADAM8 Flag tag expression construct [86], and after 48 h, cells were lysed in KEB buffer (50 mM Tris pH8, 137 mM NaCl, 2 mM EDTA, 0.5% NP40, 10 mM Phenanthroline, hr Holding GmbH), PhosStop™ (Roche Deutschland Holding GmbH). A monoclonal Flag M2 antibody (# F3165, Sigma-Aldrich Inc.) or mouse IgG (Sigma-Aldrich Inc.) was covalently coupled to magnetic beads using the Dynabeads™ antibody coupling kit (# 14311D, Invitrogen AG). The cell lysates were incubated with the beads for 2 h at 4 °C, followed by three wash steps with lysis buffer. SDS-PAGE loading buffer including DTT was added to the beads and the samples were heated up to 95 °C for 5 min to elute the bounded proteins. The samples were analyzed by SDS-PAGE and immunoblotting using specific antibodies for ADAM8 (AF1031) and ADAM17 (A300D).

For co-immunoprecipitation of mADAM17 and murine ADAM8, ADAM10$^{-/-}$; 17$^{-/-}$ HEK293T cells were transiently transfected as described above. After 48 h, cells were harvested and lysed in 450 µl lysis buffer (cOmplete™ protease inhibitor cocktail, 120 mM NaCl, 50 mM Tris, 0.5% NP-40, pH 7.4). The cell lysate was filled up to 1 ml with PBS and anti-myc antibody (# 2276, Cell-Signaling Technology, Inc.) added over night at 4 °C. In addition, Pierce™ Protein G Agarose beads were washed with PBS three times, centrifuged (1000×*g*, 3 min, 4 °C), and incubated with 3% BSA/TBS over night at 4 °C. The next day, 50 µl of blocked beads were added to the sample and incubated for 30 min at 4 °C. After centrifugation (1000×*g*, 3 min, 4 °C), beads were washed several times with lysis buffer. After the addition of SDS-PAGE loading buffer including DTT beads were heated up to 65 °C for 30 min and analyzed by SDS-PAGE and immunoblotting.

Cell lysis, SDS-PAGE, and immunoblot analysis

Cells were harvested in ice-cold PBS and centrifuged at 1100×*g* for 5 min at 4 °C. Cell pellets were washed three times with PBS and resuspended in lysis buffer [cOmplete™ protease inhibitor cocktail, 1% (v/v) Triton-X 100, PBS, pH 7.4] and incubated for 45 min at 4 °C. After centrifugation for 15 min at 15,000×*g* at 4 °C, the protein amount of lysates was determined using the BCA protein assay kit (Thermo Fisher Scientific Inc.). For a comparable analysis of possible shedding events, supernatants were normalized to the protein content of the respective cell lysates and analyzed by immunoblotting.

For separation by SDS-PAGE, protein samples were boiled in sample buffer containing DTT. After blotting transfer, nitrocellulose or PVDF membranes were saturated with 5% dry milk or 3% BSA for 1 h at room temperature. Then, membranes were incubated with the primary antibody at 4 °C overnight. The following primary antibodies were used for detection: anti-GAPDH (# 2118; Cell-Signaling Technology, Inc.), anti-actin (# A2066; Sigma-Aldrich, Inc.), anti-β tubulin (# NB600-936; Novus Biologicals, LLC), anti-ADAM10 (# 124695; Abcam plc.), anti-mADAM17 (polyclonal, generated against ectodomain), anti-hADAM17 (A300D, generated against disintegrin domain), C-terminal anti-ADAM17 (# AB19027, Merck Merck KGaA), anti-hADAM8 (# PA5-47047, Thermo Fisher Scientific Inc.), anti-meprin β (polyclonal Ab, generated against ectodomain), anti-APP (IC16, monoclonal, detecting amino acids 1–8 of Aβ [87], anti-sAPPα (14D6, monoclonal, directed against amino acids 11–16 of Aβ [88], C-terminal anti-APP (CT15, polyclonal, corresponding to amino acids 680–695 of APP695) [89], anti-N-cadherin (# EPR1791; Abcam plc.), anti-Myc (# 2276, Cell-Signaling Technology, Inc.), anti-Strep (# 34850, QIAGEN GmbH), and anti-HA (# C29F4, Cell-Signaling Technology, Inc.). Horseradish peroxidase-conjugated secondary antibodies (Thermo Fisher Scientific Inc.) were added in 5% dry milk/TBS for 1 h at room temperature and chemiluminescence detected using the Super Signal™ West Femto kit or SuperSignal™ West Pico PLUS kit (Thermo Fisher Scientific Inc.) with the LAS-3000 Imaging System (FUJIFILM Europe GmbH).

Homology modelling

Model of murine ADAM10 (UniProt accession O35598, aa residue 215–673) was built based on the crystal structure of human ADAM10 (PDB: 6BE6) using the SWISS-MODEL workspace [90]. Structure visualization and analysis were carried out using PyMOL (Schrödinger LLC).

Protein–protein interaction network analysis

For protein–protein interaction analysis and visualization, the Cytoscape software with an implemented stringApp was used [58, 91]. The STRING database was queried with TAILS-identified substrates, TIMP-1, TIMP-3, meprin β, APP, and ADAM10/17 with a confidence cutoff score of 0.5, while 14 additional interacting proteins were accepted. Missing but experimentally confirmed interactions or shedding activities were manually integrated into the map: shedding of meprin β by ADAM10/17 [54–57], APP shedding by meprin β [75], BMP1–PCPE-1 interaction [92], BMP1–FN interaction [93], and TIMP-1 inhibition of ADAM10 [71].

Acknowledgements We thank William C. Claycomb (Department of Biochemistry and Molecular Biology, Louisiana State University Health Sciences Center, New Orleans, Louisiana) for providing HL-1 cells. We thank Björn Rabe from the Biochemical Institute of the University of Kiel for ADAM10$^{-/-}$; 17$^{-/-}$ HEK293T cells.

Author contributions Conceptualization, FS and CB-P; methodology, investigation, and data analysis, FS, AH, MS, JB, US, FP, RW, MB, DS-A, SR-J, CM, SFL, CUP, JWB, AT, and CB-P; writing, FS and CB-P.

Funding This work was supported by the Deutsche Forschungsgemeinschaft (DFG) SFB 877 (Proteolysis as a Regulatory Event in Pathophysiology, Projects A1, A9, A15 and Z2), BE 4086/2-2 (C.B.-P.), University of Lyon (C.M.), FOR2290 (S.F.L.), PI379/5-2 (C.U.P.), and BA1606/3-1 (J.W.B).

MS data The mass spectrometry proteomics data have been deposited to the ProteomeXchange Consortium via the PRIDE [95] partner repository with the data set identifier PXD013718.

References

1. Hartmann M, Herrlich A, Herrlich P (2013) Who decides when to cleave an ectodomain? Trends Biochem Sci 38(3):111–120
2. Weber S, Saftig P (2012) Ectodomain shedding and ADAMs in development. Development 139(20):3693–3709
3. Duffy MJ et al (2009) The role of ADAMs in disease pathophysiology. Clin Chim Acta 403(1–2):31–36
4. Lichtenthaler SF, Lemberg MK, Fluhrer R (2018) Proteolytic ectodomain shedding of membrane proteins in mammals-hardware, concepts, and recent developments. EMBO J 37(15):e99456
5. Hayashida K et al (2010) Molecular and cellular mechanisms of ectodomain shedding. Anat Rec (Hoboken) 293(6):925–937
6. Edwards DR, Handsley MM, Pennington CJ (2008) The ADAM metalloproteinases. Mol Aspects Med 29(5):258–289
7. Takeda S (2016) ADAM and ADAMTS family proteins and snake venom metalloproteinases: a structural overview. Toxins (Basel) 8(5):155
8. Giebeler N, Zigrino P (2016) A disintegrin and metalloprotease (ADAM): historical overview of their functions. Toxins (Basel) 8(4):122

9. Reiss K, Saftig P (2009) The "a disintegrin and metalloprotease" (ADAM) family of sheddases: physiological and cellular functions. Semin Cell Dev Biol 20(2):126–137
10. Janes PW et al (2005) Adam meets Eph: an ADAM substrate recognition module acts as a molecular switch for ephrin cleavage in trans. Cell 123(2):291–304
11. Pruessmeyer J, Ludwig A (2009) The good, the bad and the ugly substrates for ADAM10 and ADAM17 in brain pathology, inflammation and cancer. Semin Cell Dev Biol 20(2):164–174
12. Zunke F, Rose-John S (2017) The shedding protease ADAM17: physiology and pathophysiology. Biochim Biophys Acta 1864(11 Pt B):2059–2070
13. Matthews AL et al (2017) Regulation of A disintegrin and metalloproteinase (ADAM) family sheddases ADAM10 and ADAM17: the emerging role of tetraspanins and rhomboids. Platelets 28(4):333–341
14. Saftig P, Reiss K (2011) The "A Disintegrin And Metalloproteases" ADAM10 and ADAM17: novel drug targets with therapeutic potential? Eur J Cell Biol 90(6–7):527–535
15. Wetzel S, Seipold L, Saftig P (2017) The metalloproteinase ADAM10: a useful therapeutic target? Biochim Biophys Acta 1864(11 Pt B):2071–2081
16. Scheller J et al (2011) ADAM17: a molecular switch to control inflammation and tissue regeneration. Trends Immunol 32(8):380–387
17. Peschon JJ et al (1998) An essential role for ectodomain shedding in mammalian development. Science 282(5392):1281–1284
18. Hartmann D et al (2002) The disintegrin/metalloprotease ADAM 10 is essential for Notch signalling but not for alpha-secretase activity in fibroblasts. Hum Mol Genet 11(21):2615–2624
19. Chalaris A et al (2010) Critical role of the disintegrin metalloprotease ADAM17 for intestinal inflammation and regeneration in mice. J Exp Med 207(8):1617–1624
20. Zhang C et al (2010) Adam10 is essential for early embryonic cardiovascular development. Dev Dyn 239(10):2594–2602
21. Shi W et al (2003) TACE is required for fetal murine cardiac development and modeling. Dev Biol 261(2):371–380
22. Jackson LF et al (2003) Defective valvulogenesis in HB-EGF and TACE-null mice is associated with aberrant BMP signaling. EMBO J 22(11):2704–2716
23. Satoh M et al (2000) Expression of tumor necrosis factor-alpha-converting enzyme and tumor necrosis factor-alpha in human myocarditis. J Am Coll Cardiol 36(4):1288–1294
24. Fedak PW et al (2006) Altered expression of disintegrin metalloproteinases and their inhibitor in human dilated cardiomyopathy. Circulation 113(2):238–245
25. Arndt M et al (2002) Altered expression of ADAMs (A Disintegrin And Metalloproteinase) in fibrillating human atria. Circulation 105(6):720–725
26. Fan D et al (2015) Cardiomyocyte A disintegrin and metalloproteinase 17 (ADAM17) is essential in post-myocardial infarction repair by regulating angiogenesis. Circ Heart Fail 8(5):970–979
27. Akatsu T et al (2003) Increased mRNA expression of tumour necrosis factor-alpha and its converting enzyme in circulating leucocytes of patients with acute myocardial infarction. Clin Sci (Lond) 105(1):39–44
28. Tousseyn T et al (2009) ADAM10, the rate-limiting protease of regulated intramembrane proteolysis of Notch and other proteins, is processed by ADAMS-9, ADAMS-15, and the gamma-secretase. J Biol Chem 284(17):11738–11747
29. Groth E et al (2016) Stimulated release and functional activity of surface expressed metalloproteinase ADAM17 in exosomes. Biochim Biophys Acta 1863(11):2795–2808
30. Sun Q et al (2014) Increased plasma TACE activity in subjects with mild cognitive impairment and patients with Alzheimer's disease. J Alzheimers Dis 41(3):877–886
31. Bertram A et al (2015) Circulating ADAM17 level reflects disease activity in proteinase-3 ANCA-associated vasculitis. J Am Soc Nephrol 26(11):2860–2870
32. Kleifeld O et al (2010) Isotopic labeling of terminal amines in complex samples identifies protein N-termini and protease cleavage products. Nat Biotechnol 28(3):281–288
33. Conrad C et al (2018) ADAM8 expression in breast cancer derived brain metastases: functional implications on MMP-9 expression and transendothelial migration in breast cancer cells. Int J Cancer 142(4):779–791
34. Hundhausen C et al (2003) The disintegrin-like metalloproteinase ADAM10 is involved in constitutive cleavage of CX3CL1 (fractalkine) and regulates CX3CL1-mediated cell-cell adhesion. Blood 102(4):1186–1195
35. Schlomann U et al (2015) ADAM8 as a drug target in pancreatic cancer. Nat Commun 6:6175
36. Jiang J et al (2011) Ectodomain shedding and autocleavage of the cardiac membrane protease corin. J Biol Chem 286(12):10066–10072
37. Prudova A et al (2016) TAILS N-terminomics and proteomics show protein degradation dominates over proteolytic processing by cathepsins in pancreatic tumors. Cell Rep 16(6):1762–1773
38. Tucher J et al (2014) LC-MS based cleavage site profiling of the proteases ADAM10 and ADAM17 using proteome-derived peptide libraries. J Proteome Res 13(4):2205–2214
39. Caescu CI, Jeschke GR, Turk BE (2009) Active-site determinants of substrate recognition by the metalloproteinases TACE and ADAM10. Biochem J 424(1):79–88
40. Seegar TCM et al (2017) Structural basis for regulated proteolysis by the alpha-secretase ADAM10. Cell 171(7):1638–1648 e7
41. Li L, Zhao Q, Kong W (2018) Extracellular matrix remodeling and cardiac fibrosis. Matrix Biol 68:490–506
42. Frolova EG et al (2012) Thrombospondin-4 regulates fibrosis and remodeling of the myocardium in response to pressure overload. Faseb J 26(6):2363–2373
43. Radice GL et al (1997) Developmental defects in mouse embryos lacking N-cadherin. Dev Biol 181(1):64–78
44. Turk V, Stoka V, Turk D (2008) Cystatins: biochemical and structural properties, and medical relevance. Front Biosci 13:5406–5420
45. Pixley FJ, Stanley ER (2004) CSF-1 regulation of the wandering macrophage: complexity in action. Trends Cell Biol 14(11):628–638
46. Hohensinner PJ et al (2007) Macrophage colony stimulating factor expression in human cardiac cells is upregulated by tumor necrosis factor-alpha via an NF-kappaB dependent mechanism. J Thromb Haemost 5(12):2520–2528
47. Reiss K et al (2005) ADAM10 cleavage of N-cadherin and regulation of cell-cell adhesion and beta-catenin nuclear signalling. EMBO J 24(4):742–752
48. Lammich S et al (1999) Constitutive and regulated alpha-secretase cleavage of Alzheimer's amyloid precursor protein by a disintegrin metalloprotease. Proc Natl Acad Sci USA 96(7):3922–3927
49. Kuhn PH et al (2010) ADAM10 is the physiologically relevant, constitutive alpha-secretase of the amyloid precursor protein in primary neurons. EMBO J 29(17):3020–3032
50. Jorissen E et al (2010) The disintegrin/metalloproteinase ADAM10 is essential for the establishment of the brain cortex. J Neurosci 30(14):4833–4844

51. Hedrich J et al (2010) Fetuin-A and Cystatin C are endogenous inhibitors of human meprin metalloproteases. Biochemistry 49(39):8599–8607
52. Buxbaum JD et al (1998) Evidence that tumor necrosis factor alpha converting enzyme is involved in regulated alpha-secretase cleavage of the Alzheimer amyloid protein precursor. J Biol Chem 273(43):27765–27767
53. Allinson TM et al (2003) ADAMs family members as amyloid precursor protein alpha-secretases. J Neurosci Res 74(3):342–352
54. Herzog C et al (2014) ADAM10 is the major sheddase responsible for the release of membrane-associated meprin A. J Biol Chem 289(19):13308–13322
55. Hahn D et al (2003) Phorbol 12-myristate 13-acetate-induced ectodomain shedding and phosphorylation of the human meprin-beta metalloprotease. J Biol Chem 278(44):42829–42839
56. Jefferson T et al (2013) The substrate degradome of meprin metalloproteases reveals an unexpected proteolytic link between meprin beta and ADAM10. Cell Mol Life Sci 70(2):309–333
57. Wichert R et al (2017) Mucus detachment by host metalloprotease meprin beta requires shedding of its inactive pro-form, which is abrogated by the pathogenic protease RgpB. Cell Rep 21(8):2090–2103
58. Szklarczyk D et al (2017) The STRING database in 2017: quality-controlled protein-protein association networks, made broadly accessible. Nucleic Acids Res 45(D1):D362–D368
59. Scharfenberg F et al (2019) Regulation of the alternative β-secretase meprin β by ADAM-mediated shedding. Cell Mol Life Sci. https://doi.org/10.1007/s00018-019-03179-1
60. Saftig P, Lichtenthaler SF (2015) The alpha secretase ADAM10: a metalloprotease with multiple functions in the brain. Prog Neurobiol 135:1–20
61. Doedens JR, Black RA (2000) Stimulation-induced down-regulation of tumor necrosis factor-alpha converting enzyme. J Biol Chem 275(19):14598–14607
62. Marcello E et al (2013) Endocytosis of synaptic ADAM10 in neuronal plasticity and Alzheimer's disease. J Clin Invest 123(6):2523–2538
63. Stoeck A et al (2006) A role for exosomes in the constitutive and stimulus-induced ectodomain cleavage of L1 and CD44. Biochem J 393(Pt 3):609–618
64. Moss ML et al (2011) ADAM9 inhibition increases membrane activity of ADAM10 and controls alpha-secretase processing of amyloid precursor protein. J Biol Chem 286(47):40443–40451
65. Jiang H et al (2011) Elevated CSF levels of TACE activity and soluble TNF receptors in subjects with mild cognitive impairment and patients with Alzheimer's disease. Mol Neurodegener 6:69
66. Conrad C et al (2017) Profiling of metalloprotease activities in cerebrospinal fluids of patients with neoplastic meningitis. Fluids Barriers CNS 14(1):22
67. Bostanci N et al (2008) Tumor necrosis factor-alpha-converting enzyme (TACE) levels in periodontal diseases. J Dent Res 87(3):273–277
68. Li X et al (2008) A tumor necrosis factor-alpha-mediated pathway promoting autosomal dominant polycystic kidney disease. Nat Med 14(8):863–868
69. Maskos K et al (1998) Crystal structure of the catalytic domain of human tumor necrosis factor-alpha-converting enzyme. Proc Natl Acad Sci USA 95(7):3408–3412
70. Arpino V, Brock M, Gill SE (2015) The role of TIMPs in regulation of extracellular matrix proteolysis. Matrix Biol 44–46:247–254
71. Amour A et al (2000) The in vitro activity of ADAM-10 is inhibited by TIMP-1 and TIMP-3. FEBS Lett 473(3):275–279
72. Amour A et al (1998) TNF-alpha converting enzyme (TACE) is inhibited by TIMP-3. FEBS Lett 435(1):39–44
73. Jagdeo JM et al (2018) N-Terminomics TAILS identifies host cell substrates of poliovirus and coxsackievirus B3 3C proteinases that modulate virus infection. J Virol 92(8):e02211-17
74. Schlage P et al (2014) Time-resolved analysis of the matrix metalloproteinase 10 substrate degradome. Mol Cell Proteomics 13(2):580–593
75. Jefferson T et al (2011) Metalloprotease meprin beta generates nontoxic N-terminal amyloid precursor protein fragments in vivo. J Biol Chem 286(31):27741–27750
76. Arnold P et al (2017) Meprin metalloproteases generate biologically active soluble interleukin-6 receptor to induce trans-signaling. Sci Rep 7:44053
77. Schutte A et al (2014) Microbial-induced meprin beta cleavage in MUC2 mucin and a functional CFTR channel are required to release anchored small intestinal mucus. Proc Natl Acad Sci USA 111(34):12396–12401
78. Cavadas M et al (2017) Phosphorylation of iRhom2 controls stimulated proteolytic shedding by the metalloprotease ADAM17/TACE. Cell Rep 21(3):745–757
79. Oikonomidi I et al (2018) iTAP, a novel iRhom interactor, controls TNF secretion by policing the stability of iRhom/TACE. Elife 7:e35032
80. Riethmueller S et al (2016) Cleavage site localization differentially controls interleukin-6 receptor proteolysis by ADAM10 and ADAM17. Sci Rep 6:25550
81. Becker C et al (2003) Differences in the activation mechanism between the alpha and beta subunits of human meprin. Biol Chem 384(5):825–831
82. Peters F et al (2019) Tethering soluble meprin α in an enzyme complex to the cell surface affects IBD-associated genes. FASEB J 33(6):7490–7504
83. Becker-Pauly C et al (2007) The α and β subunits of the metalloprotease meprin are expressed in separate layers of human epidermis, revealing different functions in keratinocyte proliferation and differentiation. J Invest Dermatol 127(5):1115–1125
84. Prudova A et al (2010) Multiplex N-terminome analysis of MMP-2 and MMP-9 substrate degradomes by iTRAQ-TAILS quantitative proteomics. Mol Cell Proteomics 9(5):894–911
85. Blanc G et al (2007) Insights into how CUB domains can exert specific functions while sharing a common fold: conserved and specific features of the CUB1 domain contribute to the molecular basis of procollagen C-proteinase enhancer-1 activity. J Biol Chem 282(23):16924–16933
86. Schlomann U et al (2002) The metalloprotease disintegrin ADAM8. Processing by autocatalysis is required for proteolytic activity and cell adhesion. J Biol Chem 277(50):48210–48219
87. Richter L et al (2010) Amyloid beta 42 peptide (Abeta42)-lowering compounds directly bind to Abeta and interfere with amyloid precursor protein (APP) transmembrane dimerization. Proc Natl Acad Sci USA 107(33):14597–14602
88. Colombo A et al (2013) Constitutive alpha- and beta-secretase cleavages of the amyloid precursor protein are partially coupled in neurons, but not in frequently used cell lines. Neurobiol Dis 49:137–147
89. Soriano S et al (2001) The amyloidogenic pathway of amyloid precursor protein (APP) is independent of its cleavage by caspases. J Biol Chem 276(31):29045–29050
90. Waterhouse A et al (2018) SWISS-MODEL: homology modelling of protein structures and complexes. Nucleic Acids Res 46(W1):W296–W303
91. Shannon P et al (2003) Cytoscape: a software environment for integrated models of biomolecular interaction networks. Genome Res 13(11):2498–2504

92. Bekhouche M et al (2010) Role of the netrin-like domain of procollagen C-proteinase enhancer-1 in the control of metalloproteinase activity. J Biol Chem 285(21):15950–15959
93. Huang G et al (2009) Fibronectin binds and enhances the activity of bone morphogenetic protein 1. J Biol Chem 284(38):25879–25888
94. Colaert N et al (2009) Improved visualization of protein consensus sequences by iceLogo. Nat Methods 6(11):786–787
95. Perez-Riverol Y et al (2019) The PRIDE database and related tools and resources in 2019: improving support for quantification data. Nucleic Acids Res 47(D1):D442–D450